Appl Biochem Biotechnol (2009) 158:605–614
DOI 10.1007/s12010-008-8410-1

Molecular Cloning and Expression Analysis of an *Mn-SOD* Gene from *Nelumbo nucifera*

Chen Dong · Guolin Li · Zhuoqi Li · Honglin Zhu · Mingquan Zhou · Zhongli Hu

Received: 24 June 2008 / Accepted: 23 October 2008 /
Published online: 19 November 2008

Abstract A rapid amplification cDNA end (RACE) assay was established to achieve the complete sequence of mitochondrial manganese-superoxide dismutase (Mn-SOD) cDNA in *Nelumbo nucifera*. The obtained full-length cDNA of *Mn-SOD* was 926 bp and contained a 699-bp open reading frame encoding an Mn-SOD precursor of 233 amino acids. The recombinant of Mn-SOD expressed by PET-32a vector in *Escherichia coli* BL21 was confirmed by sodium dodecyl sulfate polyacrylamide gel electrophoresis and Western blotting assays. A 3D structural model of the Mn-SOD was constructed by homology modeling. Real-time polymerase chain reaction analysis revealed that *Mn-SOD* mRNA was expressed in young leaves, blossom, stems, and terminal buds during reproductive stage but with the highest expression in young leaves. This significant difference demonstrated the differential expression of Mn-SOD in various organs of *N. nucifera*.

Keywords Mn-SOD · RACE · Prokaryotic expression · Homology model · Real-time PCR

Abbreviations

Mn-SOD	mitochondrial manganese-superoxide dismutase
SOD	superoxide dismutase
ROS	reactive oxygen species
RACE	rapid amplification cDNA end
IPTG	isopropylthio-*b*-D-galactoside

C. Dong · G. Li · Z. Li · H. Zhu · Z. Hu (✉)
Key Lab of the Ministry of Education for Plant Developmental Biology, College of Life Science, Wuhan University, Wuhan 430072, China
e-mail: huzhongli@whu.edu.cn

M. Zhou
Lotus Center, Wuhan University, Wuhan 430072, China

Introduction

Reactive oxygen species (ROS) such as superoxide anion ($O_2^{-\cdot}$), hydroxyl radical (·OH), and hydrogen peroxide (H_2O_2), normally generated by normal cell metabolism and chemical or environmental stresses, could cause the peroxidation of membrane lipids, breakage of DNA strands, and inactivation of enzymes [1]. In order to prevent oxidative stress, organisms had evolved a complex antioxidant system composing of nonenzymic and enzymic mechanisms to scavenge ROS [2]. Among antioxidant enzymes, superoxide dismutases (SODs) were a group of metalloenzymes that protected cells from superoxide radicals by catalyzing the dismutation of the superoxide radical to molecular O_2 and H_2O_2. SODs were classified according to their metal cofactor and their subcellular localization [3]. The predominant forms were Mn-SOD, Fe-SOD, and *Cu-Z*n-SOD. Mn-SOD and Fe-SOD were mainly found in mitochondria and chloroplast, respectively, whereas Cu-Zn-*SOD* was usually located in cytosol or chloroplast. The transgenic tobacco proved that the overexpression of the Mn-SOD in chloroplasts and mitochondria could reduce cellular damage mediated by oxygen radicals [4]. Some factors could influence the expression of SODs. For examples, drought and cold could regulate the expression of *Mn-SOD* and *Cu-Zn-SOD* gene in wheat [1]; at the same time, the age of leaves could affect the activity and mRNA level of *SODs* in wheat [5] and tobacco [6].

Nelumbo nucifera is an ancient species and a native of China, Japan, and India. As an important economic aquatic plant, its seeds and rhizomes are the traditional food in Asia area and the leaves are usually used as the herbs to treat tissue inflammation, cancer, antiemetic, skin diseases, leprosy, and food poisoning. Morphological studies revealed that it shared some characters of both dicotyledons and monocots [7]. In *N. nucifera*, only the complete sequences of *Cu-Zn-SOD* and partial *Fe-SOD* cDNA were cloned and they all consisted of multiple transcripts. But there were few reports about the different expression of *Mn-SOD* transcripts in various parts of *N. nucifera*. In this study, the complete sequence of *Mn-SOD* cDNA of *N. nucifera* was cloned and expressed in *Escherichia coli* BL21. The physical structure and homology model for Mn-SOD were generated to gain an understanding of the possible mechanisms of gene regulation. Moreover, semiquantitative real-time polymerase chain reaction (PCR) was used to compare the levels of *Mn-SOD* mRNA in four different parts at its reproductive phase.

Materials and Methods

Plant Material

N. nucifera was kept in the Lotus Research Center of Wuhan University, China. Fresh materials such as terminal buds, blossom, stems, and young leaves were collected and put into liquid nitrogen immediately, at the time when the blossom had appeared for 3 weeks.

RNA Extraction and Reverse Transcription

Total RNAs were isolated from the fresh materials of four different parts using an RNAprep Plant Kit (Tiangen Biotech Co., LTD). For synthesis of first-strand cDNA, RNAs were

firstly incubated for 5 min at 70 °C with olig(dT)$_{17}$, and then the reverse transcription was performed by M-MLV Reverse Transcriptase (Promega) for 1 h at 42 °C. The reaction mixture (total 25 μL) consisted of 3 μL RNA, 2 μL olig(dT)$_{17}$ (10 mmol/L), 5 μL M-MLV 5× reaction buffer, 3 μL dNTP, 10 μL nuclease-free water, and 2 μL M-MLV Reverse Transcriptase. The cDNA was diluted and stored at −20 °C until used.

Clone the Complete Sequence of *Mn-SOD* cDNA by 3′RACE

Based on conservative amino acid sequences, the degenerate primer pair (forward primer: 5′-CGAGCAGCCATGGCNCTBCG-3′; reverse primer: 5′-GTAYTGWARRT AGTANGCRT -3′) was designed to amplify 5′ partial cDNA of *Mn-SOD* using first-strand cDNA above as the template. The settings for the thermal profile included an initial denaturing at 94 °C for 5 min, followed by 35 cycles of 94 °C for 30 s, 50 °C for 30 s, and 72 °C for 1 min and a finally extension at 72 °C for 10 min. The fragment was ligated into pGEM-T vector (Promega) and the product of ligation was transformed into competent *E. coli* DH5α, and the 5′ partial fragment was sequenced (GenBank accession no. DQ167199).

To determine the complete sequence of the *Mn-SOD* cDNA, 3′ rapid amplification cDNA end (RACE) was performed by using BD SMART™ RACE cDNA Amplification Kit (BD Biosciences Clontech). The total RNAs from young leaves were used as the template to generate 3′ end cDNA of *Mn-SOD*, the 3′ RACE fragment was amplified by using universal primer mix (BD Biosciences Clontech) and a gene-specific primer (5′-CGAGCAGCCATGGCCTTGCG-3′), which was designed according to the 5′ partial sequence amplified (see above). The procedures were the same as 5′ partial cDNA amplification. The whole sequence was cloned and sequenced (GenBank accession no. DQ167200). The plasmid of the whole sequence was purified and stored at −20 °C.

Prokaryotic Expression

Using the plasmid above as a template, primers (forward primer: 5′-CGGAGC CATGTGCCTTGCGATCTG-3′; reverse primer: 5′-CGAAG CTTTTACCTTGATTC GGGGTG-3′) were designed to amplify the whole encoding sequence of *Mn-SOD* cDNA. The 5′ end of primers contained a restriction endonuclease site of *Sac*I and *Hin*dIII, respectively. Prokaryotic expression and western blotting were performed according to the published protocols [8]. Finally, these *E. coli* BL21 transformed were induced by isopropylthio-*b*-D-galactoside (IPTG) at various concentrations of 1.0, 0.5, and 0.1 mmol/L.

Bioinformatic Analyses of Mn-SOD

According to Baek et al. [9], alignment of the complete sequence of *Mn-SOD* cDNA with the genomic sequence (GenBank accession no. AY934858) was used for exon and intron prediction. Subcellular location of Mn-SOD protein was identified by using ProtComp Version 6.1 program (http://linux1.softberry.com/cgi-bin/programs/proloc/protcomppl.pl). Prosite identification of *N*-glycosylation and phosphorylation sites was performed by using Ph.D. Program (http://www.predictprotein.org). Other bioinformatic analysis was performed according to the published websites [10]. A 3D structural model of Mn-SOD proteins was constructed by homology modeling according to the published protocols [11], and the Protein 1LUV [12] was used as the template.

Real-time PCR

Clone the Sequence of β-actin cDNA

The primer pair (5′-AACTGGGATGACATGGAGAA-3′ and 5′ -C T G TTGGAAGGTGCT GAGAG-3′) was designed to amplify the partial sequence of *β-actin* based on the homologous sequences of other species. The procedures were the same as the clone of *Mn-SOD*. Partial *β-actin* cDNA was cloned and sequenced (GenBank accession no. EU131153).

Mn-SOD mRNA Different Expression

Real-time PCR was carried out in a fluorimetric thermal cycler (Rotor Gene 2000; Corbett Research, Australia) using the DNA-binding dye SYBR Green I (Toyobo Co., Ltd., Osaka, Japan) for detection of PCR products. The *β-actin* was chosen as a reference gene [13]. According to the sequences cloned (see above), the primers of *Mn-SOD* (5′-AGGGT TAGGGTTTAGTCAT-3′; 5′-AGAGCCTTATTGTAGTTGGT-3′) and *β-actin* (5′-TGATCGGAATGGAAGC-3′; 5′-CAGCAATACCAGGGAAC-3′) were designed with primer-analyzing software Primer Premier 5 (Premier). The $2^{-\Delta\Delta Ct}$ methods were used to obtain relative gene expression data according to the published protocols [14]. The highest value was set as 100% and for the tested samples the values relative to this value were calculated. The reaction was done with SYBR Green real-time PCR Master Mix according to specifications. The settings for the thermal profile were as follows: initial denaturation 95 °C for 30 s, followed by 40 amplification cycles: 95 °C for 5 s, 55 °C for 10 s, and 72 °C for 15 s. The products of real-time PCR were analyzed by electrophoresis on 1% agarose–ethidium bromide gel and sequenced. All samples were run in triplicate, and the trials were repeated three times.

Results

Cloning and Analysis of *Mn-SOD* cDNA

Our results showed that only one functional form of *Mn-SOD* cDNA of *N. nucifera* was cloned in this experiment. In order to minimize erroneous nucleotide incorporation by Taq DNA polymerase, the cDNA products was sequenced five times. The whole *Mn-SOD* cDNA sequence was about 926 bp including the start code ATG and stop code TAA. Based on conceptual translation of the cDNA sequence in all three open reading frames and alignment with the known sequences of Mn-SOD proteins in GenBank database, it could be inferred that the initiation site of translation was located at nt 9. The 5′ untranslated region and 3′ untranslated region contained 9 bp and 215 bp, respectively, and the encoding sequence consisted of 699 bp. The whole gene contained six extrons and five introns. Detailed messages of introns and extrons were shown in Fig. 1.

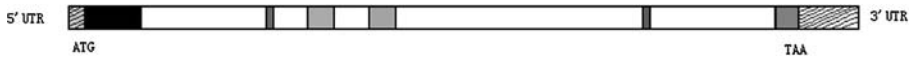

Fig. 1 Structure of the *N. nucifera Mn-SOD* gene. *Solid boxes* represented the coding sequences (extron); *open boxes* represented the noncoding sequences (intron), and *shaded boxes* indicated 5′and 3′ untranslated regions. The start code (ATG) and the stop code (TAA) were also shown

Bioinformatic Analyses of Mn-SOD

We predicted putative protein of the *Mn-SOD* and found that it contained 233 amino acids. The theoretical isoelectric point (pI) and molecular weight (m_w) of the protein sequence were 6.59 and 25,928.45 Da. A single potential *N*-glycosylation site was found at N-99 (NHSI). Two protein kinase II phosphorylation sites were located at S-8 (SRK) and S-161 (SQK) in putative protein and two casein kinase II phosphorylation sites T-29 (TLPD) and S-38 (SALE). The consensus sequence DVWEH observed in Mn-SOD was located between D-189 and H-193. And the sequence LPDL located at the N-terminal region in most eukaryotic Mn-SOD was present in the deduced protein. Four residues known to be involved in metal binding in Mn-SOD protein were found in this amino acid sequence (H-52, H-100, H-193, and D-189; Fig. 2). The predicted amino acid sequence of Mn-SOD protein exhibited the characteristic motifs of Mn-SOD family. A mitochondrial transit peptide consisting of residues 1–24 (MALRSVISRKTLGSLGLGFSHARG) was also identified in the putative protein. Compared with sequences of other species, such as *Camellia sinensis* (AAT68778), *Nicotiana plumbaginifolia* (CAA32643), *Hevea brasiliensis* (P35017), *Gossypium hirsutum* (ABA00455), *Prunus persica*(CAB56851), *Tamarix androssowii* (AAS77885), and *Digitalis lanata* (CAC05259), the identity of the putative amino acid was 67.62%.

The target protein and template protein shared a high degree of homology. It was found that human Mn-SOD (PDB code: 1LUV: A) was selected as the best structure template for the query sequence of Mn-SOD. The Ramachandran plot of the model and template was shown in Table 1. The analysis for the model presented 92.7% of residues in most favorable regions, 6.7% of residues in additional allowed regions, 0.6% of residues in generously allowed regions, and none of residues in disallowed regions. The model suggested that the N-terminal domain of Mn-SOD protein was a long alpha antiparallel hairpin and the C-terminal domain was a mixed alpha–beta fold table. These results indicated that the molecular model presented here had good overall stereochemical qualities (Fig. 3).

Prokaryotic Expression and Western Blotting

About 699-bp encoding sequence was inserted in PET-32a expression vector, and IPTG at concentration of 1.0 mmol/L efficiently induced the expression of Mn-SOD protein in this prokaryotic expression system. The amounts of Mn-SOD expression were varied during different induction time. That bacterial lysates were analyzed by SDS-PAGE and Western blotting with anti-His-tag antibody confirmed that this protein induced was a Mn-SOD fusion protein (Fig. 4).

Datum Analysis of Real-time PCR

The *R* values of both *β-actin* (0.9977) and *Mn-SOD* (0.9972) were close to 1. It indicated that the PCR system here was valid. The efficiencies of the real-time PCR procedure for the control and the *Mn-SOD* mRNA were 1.08 and 1.06, respectively; moreover, the amplification efficiency of the target was approximately equal to that of the reference. So the $2^{-\Delta\Delta Ct}$ methods could be used to analyze the relative quantity. All the products of real-time PCR were from 75 through 200 bp in size, which was exactly suitable to improve the efficiency of PCR. The data proved that there were dynamic changes for *Mn-SOD* expression in different parts. The expression level of *Mn-SOD* mRNA was highest in the leaves and lowest in the stems. The leaves, blossom, and terminal buds were correspondingly 21-, 7-, and 2.8-fold as high as stems in *Mn-SOD* expression amounts (Fig. 5).

```
CGAGCAGCCATGGCCTTGCGATCTGTCATCAGTCGGAAAACCCTCGGAAGTCTAGGGTTA      60
          M  A  L  R  S  V  I  S  R  K  T  L  G  S  L  G  L          17
GGGTTTAGTCATGCTCGGGGGTTGCAGACCTTCACGCTTCCTGATCTTCCTTACGATTAC     120
 G  F  S  H  A  R  G  L  Q  T  F  T  L  P  D  L  P  Y  D  Y       37
AGTGCTCTTGAACCCGCCATAAGTGTGGAAATTATGCGGCTCCATCACCAGAAGCACCAT     180
 S  A  L  E  P  A  I  S  V  E  I  M  R  L  H  H  Q  K  H  H       57
CAGACTTACATTACCAACTACAATAAGGCTCTTGAGCAGCTCGAGGAAGCCATGGCCAAG     240
 Q  T  Y  I  T  N  Y  N  K  A  L  E  Q  L  E  E  A  M  A  K       77
GGCGATTCGTCCGCAGTGGTTAAATTGCAGGCCGCCATCAAATTTAACGGGGGAGGGCAT     300
 G  D  S  S  A  V  V  K  L  Q  A  A  I  K  F  N  G  G  G  H       97
ATCAATCACTCTATTTTCTGGAAAAATCTCATTCCTACTAGTGAAGGAGGTGGAGAGCCC     360
 I  N  H  S  I  F  W  K  N  L  I  P  T  S  E  G  G  G  E  P      117
CCCCATGGTGCCCTTGGTTGGGCTATTGACACACATTTTGGTTCATTTGAAGCATTGGTG     420
 P  H  G  A  L  G  W  A  I  D  T  H  F  G  S  F  E  A  L  V      137
AAAAAGGTAAATGCAGAAGGTGCTGCTCTGCAAGGTTCTGGTTGGGTGTGGCTAGGCGTG     480
 K  K  V  N  A  E  G  A  A  L  Q  G  S  G  W  V  W  L  G  V      157
GATAAAGAATCACAAAAACTTGTGGTTGAAACAACAGCAAATCAGGATCCATTGGTTACC     540
 D  K  E  S  Q  K  L  V  V  E  T  T  A  N  Q  D  P  L  V  T      177
AAGGGGCCAAATTTAGTTCCTTTGCTTGGGATAGATGTGTGGGAGCATGCATACTACTTG     600
 K  G  P  N  L  V  P  L  L  G  I  D  V  W  E  H  A  Y  Y  L      197
CAGTACAAGAATGTCAGACCTGACTATCTCAATAATATATGGAAGGTTATTAACTGGAAA     660
 Q  Y  K  N  V  R  P  D  Y  L  N  N  I  W  K  V  I  N  W  K      217
TATGCTGGTGAAGTATATGACAAAGAATGCCCGCACCCCGAATCAAGGTAAAAACTTTGT     720
 Y  A  G  E  V  Y  D  K  E  C  P  H  P  E  S  R  *               233
GGTTCTCCCGCATGGATCAGGAGAGATGCCGGTTTAGAGTTGGGCAGGCAGTCTTCACGA     780
AGGGAACAATAATAATTTGTTGTGTGGATGATTAAGTTTTCTGTTTCTGCCATGGTGTAC     840
TTATCTTGGACTAGTGTACTGTTGTTAGAGATGTTTTTCCCTGCTCCAATGAATAACACA     900
ACATGTTTGCTTGTTTTATAAAAAAA                                       926
```

Fig. 2 The nucleotide acid sequence of *Mn-SOD* cDNA and its deduced amino acid sequence of Mn-SOD protein. Both nucleotide and deduced amino acid sequences were numbered at the end of each line. The deduced Mn-SOD protein sequence was shown under the cDNA sequence. Amino acid residues corresponding to metal-binding legends were *underlined*. The *asterisk* denoted the translation stop code

Table 1 Comparisons of Ramachandran plot statistics between the model and the template.

Model–template	Region of the Ramachandran plot (%)			
	Most favorable	Additional allowed	Generously allowed	Disallowed
Mn-SOD	92.7%	6.7%	0.6%	0.0
1LUV:A	90.4%	9.0%	0.6%	0.0

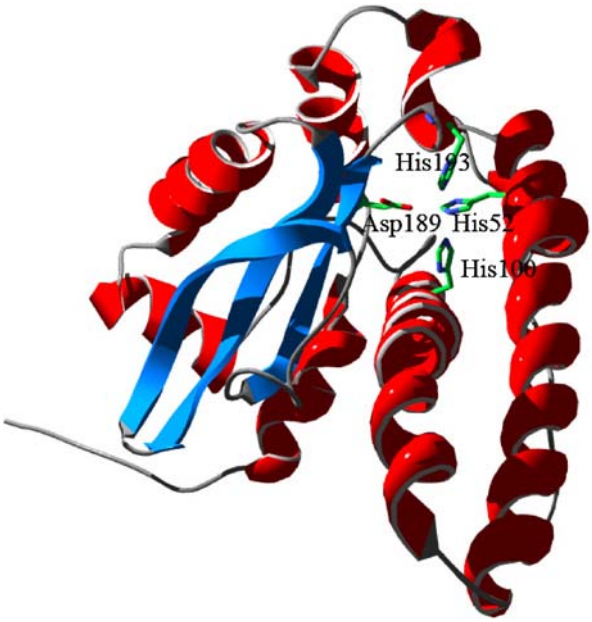

Fig. 3 Molecular modeling of the *N. nucifera* Mn-SOD protein. The residues interacting with the metal manganese were His-52, His-100, His-193, and Asp-189. The N-terminal long alpha antiparallel hairpin and the C-terminal mixed alpha–beta fold characteristics were shown

Discussion

The RACE technique allowed us to clone the complete sequence of the *Mn-SOD* targeted cDNA without needing cDNA library, which contained not only the encoding sequence but also the untranslated regions. In recent years, multiple transcripts of *Mn-SOD* had been

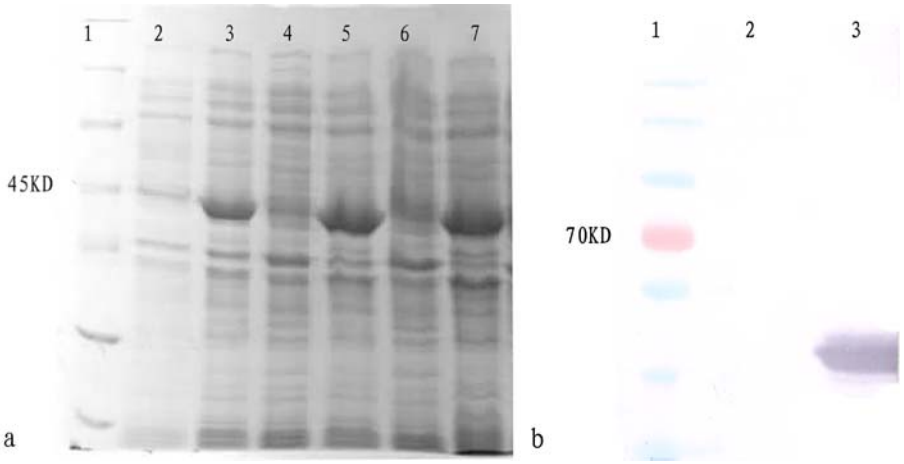

Fig. 4 **a** The amounts of Mn-SOD expression at 1.0-mmol/L concentration of IPTG during various induction times. *Lanes 2*, *4*, *6* represented the amounts of control groups induced with PET-32a during induction time (1, 2, 3 h). *Lanes 3*, *5*, and *7* represented the amounts of groups induced with PET-32a-Mn-SOD during induction time (1, 2, 3 h). *Lane 1*, molecular standard marker. **b** Total bacterial lysates were separated by SDS-PAGE, and stain of bacterial lysates induced by PET-32a (*lane 2*) and PET-32a-Mn-SOD (*lane 3*) was transferred to a membrane; filter was immunoblotted with anti-His-tag antibody. *Lane 1*, molecular standard marker

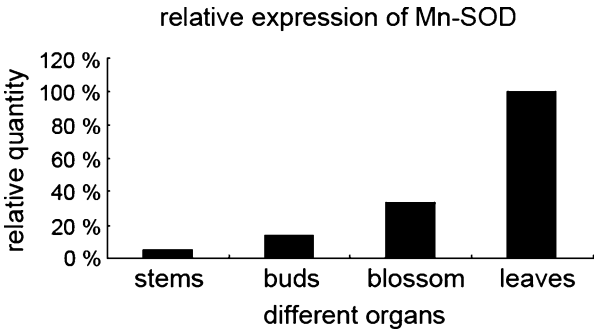

Fig. 5 Relative amounts of *Mn-SOD* mRNAs which were isolated from four different parts (stems, terminal buds, blossom, and leaves) were determined by real-time PCR. The mean numbers of PCR cycles required to obtain measurable amplification for *Mn-SOD* (stems 19.89, terminal buds 20.39, blossom 24.23, and leaves 26.84) and *β-actin* (stems 18.54, terminal buds 20.56, blossom 25.69, and leaves: 29.88) were calculated

reported in other species, and some researches proved that these multiple *Mn-SOD* transcripts might be generated by a single functional gene in rat [15] and human [16] or by a multigene family in maize [17]. Though there were several kinds of transcripts of *Fe-SOD* and *Cu-Zn-SOD* cloned in *N. nucifera* (unpublished data), only one kind of *Mn-SOD* transcript of *N. nucifera* was found in this study. Compared with the cDNA sequence (GenBank accession no. AY934858) published, the cDNA we cloned was 118 nt longer. It might be generated by alternate polyadenylation [18]. Compared with other *Mn-SOD* cDNA sequences published in other species, the homologies of the nucleotide and its putative amino acid sequences were considerable high. These data indicated that the *Mn-SOD* gene was rather conservative among the different species.

Despite the size variation of *Mn-SOD* gene, the number and order of exons and introns were the same in almost all the plants reported. All introns in *Mn-SOD* gene of *N. nucifera* started with nucleotides GT at the 5′ boundary and ended with nucleotides AG at 3′ boundary. The intron splicing followed the GU-AG rule, which was common in rubber tree, human, and wheat for the consensus sequences of splice junction sites [9].

Crystallographic studies with human had shown that metal-binding sites of Mn-SOD were located at three histidine residues and one aspartate residue [19]. The corresponding residues in *N. nucifera* were identified as H-52, H-100, H-193, and D-189. In a great degree, these residues, as well as the sequences DVWEH and LPDL, were conservative in eukaryotic species. It proved that the protein putative had the common characteristics of Mn-SOD family [10]. In addition, a prokaryotic expression system was constructed by using PET-32a as the expression vector. The recombinant protein contained a partial sequence of PET-32a (about 18.28 KDa). The molecular weight of Mn-SOD protein was similar to that predicted by ExPasy program.

Real-time PCR is proven a useful method in molecular biology researches [13]. At present, real-time PCR is increasingly being adopted for RNA quantification and genetic analysis. The data of semiquantification PCR showed that leaves expressed *Mn-SOD* on a relatively high level within the tested organs of *N. nucifera* during the reproduction phase. Both chloroplast and mitochondria were mainly resources of ROS through electron-transport chain of photosynthesis [2] and respiration [20, 21]; and Mn-SOD activity paralleled the activity of electron-transport chain of mitochondria [22]. The leaves were mainly organs of photosynthesis and respiration. Higher mRNA levels of *Mn-SOD* gene in young leaves suggested that the higher amount of Mn-SOD might be able to eliminate the

ROS within the tested organs. Its induction could be considered as a response against superoxide radicals generated in the mitochondria. We also thought that high-level expression of the *Mn-SOD* in the leaves probably was propitious to delay their senescence, so that during the reproduction stage the leaves could provide enough nourishment to the stems or rhizomata during the asexual reproduction phase.

At the same time, the environment also affected the expression of *Mn-SOD*. Because of plenty of oxygen above the water for respiration, the leaves and blossom could produce much more ROS than the terminal buds and stems under the water. The expression of *SODs* was coordinately regulated by the oxygen tension in *N. nucifera* [23]. The levels of SODs were enhanced under hyperoxia and that they were repressed under anoxia and hypoxia. In addition, leaves living above water were relatively easier to be attacked by pathogen, insects, and environment factors such as the temperature and wounding than those organs under water [24]. Therefore, as a general mechanism to protect plants themselves from these disadvantageous influences, leaves and blossom remained with higher levels of SODs including Mn-SOD than terminal buds and stems did. In a word, the physiological development and surroundings lived in coordinately determined the different expression of *Mn-SOD* gene in the organs of *N. nucifera*. In fact, the various parts of *N. nucifera*, including leaves, stamens, and rhizomes, were proven to have high antioxidant activity [25]. And the Korean traditional lotus liquor made from blossom and leaves was proven to have relatively high antioxidant activities [26]. In this study, the levels of *Mn-SOD* mRNA were various in the different parts during reproductive stage, it demonstrated that the *Mn-SOD* gene in *N. nucifera* should be differentially expressed [17]. But our study just focused on the reproductive stage, the expression of *Mn-SOD* gene might be various during different stages. It remained to be further studied.

Acknowledgments The authors are greatly indebted to Prof. Yunchun Song and Ying Diao for critical reading of this manuscript, and doctor Hui Liu for his assistance in the laboratory work. We are especially appreciative of the reviewers for their helpful comments and detailed suggestions. This work was financially supported by the Key grant Project of Chinese Ministry of Education (no. 307018), National Science and Technology Pillar Program (no. 2007BAD37B06), and Natural Science Foundation of Hubei Provience (no. 2007ABD003)

References

1. Wu, G., Wilen, R. W., Robertson, A. J., & Gusta, L. V. (1999). *Plant Physiology*, *120*, 513–520.
2. Asada, K., & Takahashi, M. (1987). In D. J. Kyle, C. B. Osmond, & C. J. Arntzen (Eds.), *Photoinhibition* pp. 227–287. Amsterdam: Elsevier Science.
3. Bowler, C., Montagu, M. V., & Inze, D. (1992). *Annual Review of Plant Physiology and Plant Molecular Biology*, *43*, 83–116.
4. Bowler, C., Slooten, L., Vandenbranden, S., Rycke, R. D., Botterman, J., Sybesma, C., et al. (1991). *European Molecular Biology Organization Journal*, *10*, 1723–1732.
5. Casano, L. M., Martin, M., & Sabater, B. (1994). *Plant Physiology*, *106*, 1033–1039.
6. Kurepa, J., Herouart, D., Van Montagu, M., & Inze, D. (1997). *Plant and Cell Physiology*, *38*(4), 463–470.
7. Esau, K., & Kosakai, H. (1975). *Phytomorphology*, *25*, 100–112.
8. Shen, G., Pang, Y., Wu, W., Deng, Z., Liu, X., Lin, J., et al. (2005). *Plant Physiology & Biochemistry*, *43*, 836–843.
9. Baek, K. H., Skinner, D. Z., Ling, P., & Chen, X. (2006). *Genome*, *49*, 209–218.
10. Dash, B., Metz, R., Huebner, H. J., Porter, W., & Phillips, T. D. (2007). *Gene*, *387*, 93–108.
11. Zheng, Z. L., Zuo, Z. Y., Liu, Z. G., Tsai, K. C., Liu, A. F., & Zou, G. L. (2005). *Journal of Molecular Graphics and Modelling*, *23*, 373–380.
12. Hearn, A. S., Stroupe, M. E., Cabelli, D. E., Ramilo, C. A., Luba, J. P., Tainer, J. A., et al. (2003). *Biochemistry*, *42*, 2781–2789.

13. Huggett, J., Dheda, K., Bustin, S., & Zumla, A. (2005). *Genes and Immunity*, *6*, 279–284.
14. Livak, K. J., & Schmittgen, T. D. (2001). *Methods (San Diego, Calif.)*, *25*, 402–408.
15. Hurt, J., Hsu, J. L., Dougall, W. C., Visner, G. A., Burr, I. M., & Nick, H. S. (1992). *Nucleic Acids Research*, *20*(12), 2985–2990.
16. Church, S. L. (1990). *Biochimica et Biophysica Acta*, *1087*, 250–252.
17. Zhu, D., & Scandalios, J. G. (1993). *Proceedings of the National Academy of Sciences of the United States of America*, *90*, 9310–9314.
18. Carmona, M. J., Cubas, P., & Martinez-Zapater, J. M. (2002). *Plant Physiology*, *130*, 68–77.
19. Borgstahl, G. E. O., Parge, H. E., Hickey, M. J., Beyer, W. F., Hallewell, R. A., & Tainer, J. A. (1992). *Cell*, *71*, 107–118.
20. Freeman, B. A., & Crapo, J. D. (1982). *Laboratory Investigation*, *47*(5), 412–426.
21. Ksenzenko, M., Konstantinov, A. A., Khomutov, G. B., Tikhonov, A. N., & Ruuge, E. K. (1983). *Federation of European Biochemical Societies Letters*, *155*(1), 19–24.
22. Bowler, C., Alliotte, T., Bulcke, M., Bauw, G., Vandekerckhove, J., Van Montagu, M., et al. (1989). *Proceedings of the National Academy of Sciences of the United States of America*, *86*, 3237–3241.
23. Ushimaru, T., Kanematsu, S., Katayama, M., & Tsuji, H. (2001). *Physiological Plant*, *112*, 39–46.
24. Ni, X. M. (1987). *Nelumbo nucifera* pp. 66–67. Beijing: Science Press Chapter 6: The cultivation of *Nelumbo nucifera*.
25. Rai, S., Wahile, A., Mukherjee, K., Saha, B. P., & Mukherjee, P. K. (2006). *Journal of Ethnopharmacology*, *104*(3), 322–327.
26. Lee, H. K., Choi, Y. M., Noh, D. O., & Suh, H. J. (2005). *International Journal of Food Science & Technology*, *40*, 709–715.